Wojciech Jamrozik, Marek Fidali

Application of image fusion to identification of welding imperfections

Abstract: It has been presented the issues concerning the application of images fusion registered in visible and infrared radiation for diagnostics of MIG/MAG processes. The sequences of visible and infrared images visualizing the arc burning during performing the weld were examined. Recorded during experiments image sequences were subjected to fusion and next to analysis in order to obtain diagnostic signals. On the basis of selected features of diagnostic signals it was carried out the classification of the welding process state and its results were compared with those obtained for diagnostic signal features determined independently for visible and infrared images. The results show that the application of images fusion enables to identify effectively various welding imperfections forming in welding processes.

Keywords: MAG welding, welding imperfections, image fusion, identification of welding process state classification

Introduction

Obtaining diagnostic signals is an important stage of diagnosing, the primary purpose of which is to recognise the state of an object or a process. Diagnostic signals are courses of certain quantities in time, on the basis of which it is possible to distinguish states. Diagnostic signals can simply be courses registered by means of various sensors or they can be obtained by processing and analysing such courses as the courses of values of features in time. Real diagnostic tasks, carried out for objects or processes characterised by high complexity require recording many process parameters. However, it should be noted using all such parameters to generate diagnostic signals, and further, to recognise the state of an object or a process is pointless as some signals carry no information about state changes and may only bring information noise to a recognition process.

In welding process diagnostics, process parameters are mostly registered in the form of the time courses of the values of physical quantities affecting the quality of a joint, e.g. current, voltage, gas flow, sound flow etc. Recent years have seen a significant growth in the importance of visual techniques in diagnosing, as well as those of welding processes [7], which has created the possibility of recording signals in the form of image sequences. Such images are mainly recorded in the range of visible light (TV) as well as in the middle infrared band (IR, with a wavelength from approximately 0.9 to 14 μm). The use of a thermographic camera, operating in the infrared range enables a non-contact and multipoint temperature measurement. Thanks to this solution it is possible to obtain information about temperature distribution, mainly in the area of a burning arc, weld pool and a cooling weld.

dr inż. Wojciech Jamrozik (Ph.D. Eng.), dr inż. Marek Fidali (Ph.D. Eng.) - Politechnika Śląska, Wydział Mechaniczny Technologiczny, Instytut Podstaw Konstrukcji Maszyn/Silesian University of Technology, Faculty of Mechanical Engineering, Institute of Fundamentals of Machinery Design

At the same time a given object can be observed by means of IR and TV cameras. In such cases the redundant representation of objects in an image is obtained. In addition to information relevant from a welding process recognition point of view, contained in IR and TV images, there is also some redundant information. The elimination of redundant information with simultaneous maintaining of all information important from a welding imperfection recognition point of view can be obtained by an image fusion, i.e. a multi-stage technique of merging many input images, presenting the same scene as one output image [4]. Images obtained in this way can constitute the basis for determining diagnostic signals enabling efficient diagnosing of welding processes [3].

Image fusion

Image fusion is a technique which consists in forming a new synthetic image out of at least two input images recorded by devices of different parameters and different locations. It is important that input signals should represent a common scene (or its fragment). The process of image fusion is a multi-stage process and in most cases consists of three basic stages: image matching, image aggregation and post-processing, consisting mainly in spatial filtration sharpening a resultant image. Sometimes the third stage is omitted and the whole fusion includes matching and aggregation. There are three basic groups of methods enabling image fusion, i.e. methods operating on the level of pixels, methods operating on the level of features and methods operating on a symbolic level also referred to as a decision level.

In practice, the most commonly used fusion methods are those operating on the level of pixels. These methods assume the existence of a relationship between individual pixels of all input images. Such an assumption requires performing a geometric matching of input images. The results of an image fusion largely depend on the quality of the conducted matching.

Geometric matching, being the first stage of image fusion, can be carried out in several ways [5]. The most common is image matching, i.e. matching of areas characterised by similar brightness or colour or matching based on the characteristic features of an image, e.g. the edges or points of objects visible in an image. Matching images registered in visible light and in infrared is a complex task as image contents differ, usually in pixel values and object shapes. An additional problem can be the lack of an unambiguous relationship between object colours and greyness shades in visible light and object colours and greyness shades in infrared. Reference publications contain descriptions of various matching algorithms, yet comparative tests [2], [5] of selected algorithms justify the application of hybrid algorithms, making use of both the brightness distribution of areas in an image and of edge-related information. One of such methods described in the publication [5] can be used with indexed images or images recorded in the scale of greyness shades. This method uses edge orientation maps. On the basis of these maps as well as on the basis of pixel brightness values it is possible to create a 3D bar chart. An objective function determines the uncertainty of matching objects located in input images corresponding to edges as well as the shade of individual areas. Such a solution enables the obtainment of a low level of matching errors.

The next stage of the fusion of images is their aggregation aimed at joining previously matched input images into one output image. Similarly, as in the case if matching algorithms, there is also a significant number of well described algorithms for the aggregation of images. The algorithms on the level of pixels can be divided into four groups [7]: algorithms operating on a model of a colour

space, statistical/numerical algorithms, algorithms making use of a large-scale decomposition as well as spectral and radiometric algorithms. For the purpose of merging vision and thermographic images of a welding arc, the authors considered mainly algorithms using a large-scale transform, the functioning of which is based on a general scheme of successive operations presented in Figure 1.

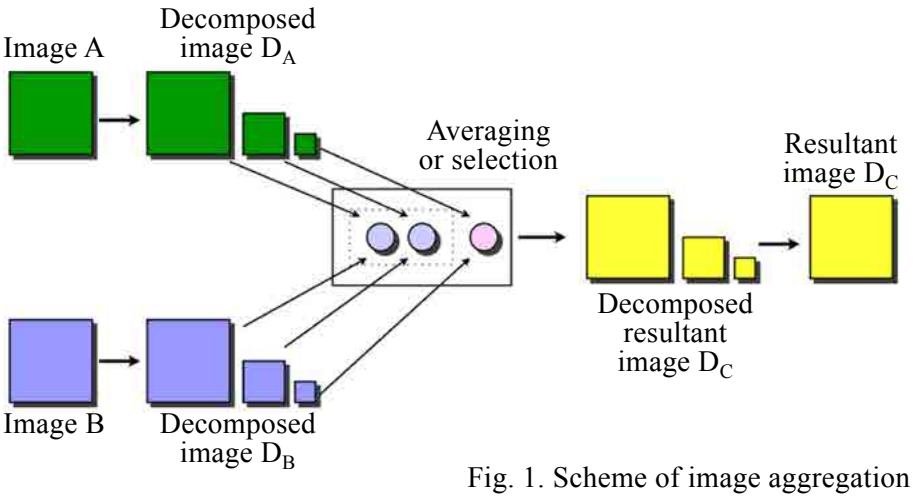

Fig. 1. Scheme of image aggregation using large-scale transformation (on the basis of [1])

As is shown in Figure 1, aggregation using large-scale transformation consists of three stages [1]:

- decomposition, when each of the input images is transformed into a hierarchical structure, whose successive stages are appropriately transformed copies of an input image,
- joining of images, during which, by means of a proper fusion principle using the selection or averaging of pixels, a resultant decomposed image representation is determined,
- synthesis, the result of which is a new synthetic image, created by using a transform reverse to the one used at the decomposition stage.

The hierarchical structure is obtained by using:

- pyramid transformation, used for determining the set of images, in which each of the images in a pyramid is two times smaller than an image on a lower level of the pyramid,
- wavelet transformation, which is similar to pyramid decomposition methods, where the main difference is the amount of information contained in the hierarchical structure of images. Pyramid transformations lead to a redundant set of transformation factors, whereas a wavelet transform leads to a non-redundant image representation.

Within the confines of previously conducted tests [3], the authors examined and assessed various aggregation algorithms for application in the fusion of welding arc vision and thermographic images.

For the purpose of the tests described in the article an aggregation algorithm based on a shift invariant Haar wavelet (SIH) [6] was used. Within this method, unlike in a discrete wavelet transform, successive image copies are not subjected to resolution reduction, which leads to obtaining a highly redundant image representation. This algorithm for joining information out of decomposed input images uses Burt's adaptive rule [1]. As a result it is possible to join images by averaging or selecting pixels depending on the changes of pixel brightness variance in some vicinity of a given pixel. The use of this method, to a significant extent, enables maintaining information about the shape, brightness distribution and temperature in the welding arc area and the weld pool.

Welding process observation

The observation of a MAG welding process was carried out using an observation head composed of an uncooled thermographic camera (Infratec VarioCam Head) with a bolometric detector of 640×480 px resolution and a lens with a focal length f=50 mm as well as a CCD camera operating in the visible

light range (ImagingSource DMK21AF04), with 640×480px resolution, equipped with a lens with a focal length *f*=25 mm. The cameras were provided with filters protecting optical systems against spatters and limiting the power of electromagnetic radiation emitted during welding. Images were recorded synchronically at a frequency of 50 images/s.

The MAG welding tests were carried out at the Department of Welding of the Silesian University of Technology, using a robotised station for rectilinear MAG welding The station was equipped with a welding tractor AS14a-1200 made by the OZAS company and provided with a set of supports for fixing a welding torch as well as with a semi-automatic welding machine TotalArc 5000 produced by Castolin. The testing station with the observation head is presented in Figure 2.

Fig. 2. Mechanised station for MAG welding

During experiments butt joints of steel S235JR (EN 10025-2) sheets with the dimensions of 300×150×5 mm were made. Apart from situations when special cases of imperfections were simulated, the edges of sheets were V-bevelled at an angle of α=60°; the distance between the sheets was *b*=1.0 mm.

The butt joints of sheets were made on a copper plate equipped with mechanical clamping of sheets being joined. The welding process involved the use of a solid electrode wire (Castolin CastoMag 45255) with a diameter of 1.2 mm and a gas mixture M21 (82%Ar+18%CO_2). Welding parameters are presented in Table 1.

Table 1. MAG welding parameters

Welding current [A]	Arc voltage [V]	Welding rate [cm/min]	Wire feeding rate [m/min]	Shielding gas flow rate [l/min]	Exposed length of wire [mm]
240	25	32	7,4	15	15

While making welded joints various welding parameters were deliberately simulated by destabilising arc using the following:

- changes in the voltage and/or current of an electric arc,
- changes in a shielding gas flow rate,
- improper preparation of the surfaces of sheets to be joined.

Welding imperfections were classified into the following 8 condition classes:

- z_0 – model process, no imperfections,
- z_1 – momentary disappearance of a gas shielding,
- z_2 – atmospheric corrosion of sheets to be joined,
- z_3 – weld groove imperfections, simulated by openings located at a specified distance from one another, in the axis of the weld groove,
- z_4 – improper welding current different by ±20% against model parameters,
- z_5 – improper distance between sheets being joined, amounting to 1.5 mm, 2.0 mm, 2.5 mm, 3.0 mm and 3.5 mm,
- z_6 – improper arc voltage, different by ±15% against model parameters,
- z_7 – changing geometry of the weld groove due to various values of a bevelling angle: 0°, 15°, 30°, 45°, 60°.

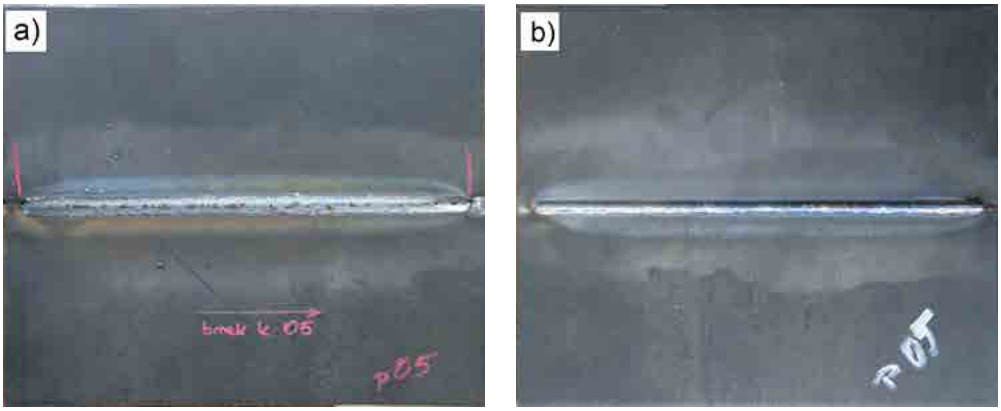

Fig. 3. Exemplary model of welded joint:
a) view from the weld face b) view from the weld root

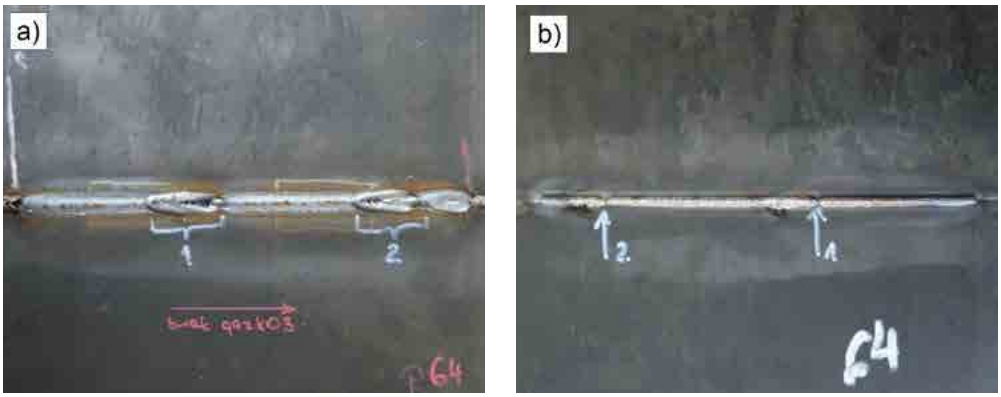

Fig. 4. Exemplary welded joint, with an imperfection caused by the momentary disappearance of the gas shielding:
a) view from the weld face b) view from the weld root

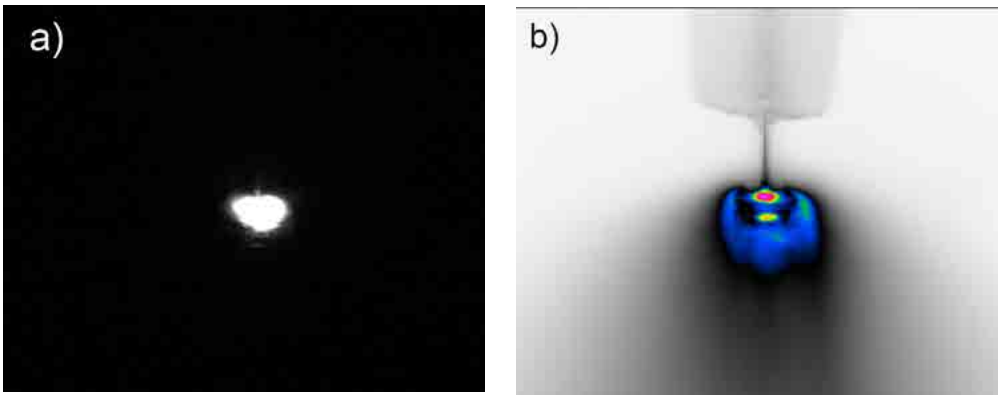

Fig. 5: Examples of images presenting a welding arc recorded:
a) in visible radiation range b) in infrared

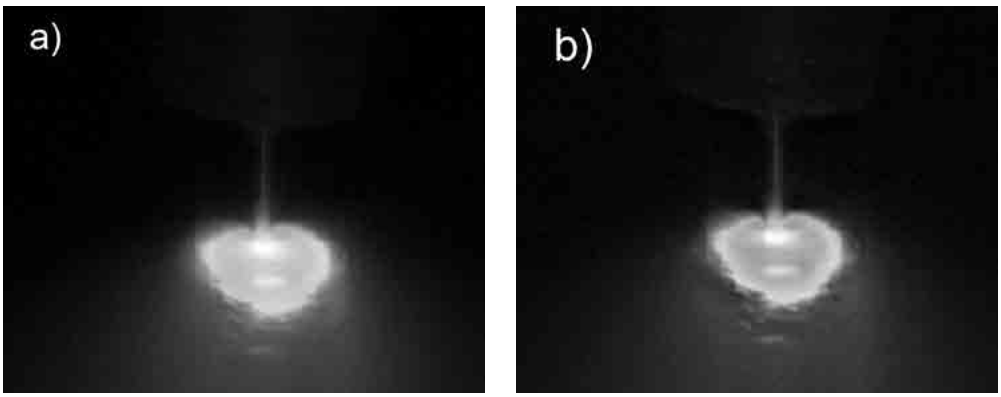

Fig. 6. Exemplary images presenting a welding arc obtained by
a) averaging b) aggregation of vision and thermographic images matched by means of the SIH method

Figures 3 and 4 present an example of a model joint and a joint formed during the disappearance of a gas shielding.

The conducted observations enabled obtaining sequences of thermographic images and images recorded in the visible light range. The examples of images showing a welding arc in visible light and in infrared are presented in Figure 5.

The recorded sequences of vision and thermographic images underwent fusion. As a result, sequences of new, i.e. post-fusion images, were obtained.

Figure 6 presents examples of post-fusion images, where the image in Figure 6a was obtained using the aforementioned aggregation algorithm based on a shift invariant discrete wavelet transform modification. In turn, for comparative purposes Figure 6b presents the effect of aggregation consisting in averaging the pixel values of input images.

Both images contain information from the vision and thermographic images, yet as can be easily seen the averaged image is out of focus. In

addition, the contrast of the area representing temperature distribution is reduced. The image obtained through SIH-based aggregation is characterised by a much higher contrast and sharpness of contours. The effect of the thermographic image on the resultant image is significant, which facilitates the description of the image both by means of measures taking into account welding arc luminous intensity and those based on temperature distribution.

Analysis of images after fusion

The new images created through fusion were analysed in order to determine the set of features used for recognising welding process states. Three types of features were determined for the specified area of interest containing the welding arc area. The first type includes first- and second-grade statistical features based on the vector of the bar chart and Co-Occurrence Matrix (COM). The features in question include the average, variance, coarseness, kurtosis, contrast, correlation, entropy etc. The second type includes topological features describing the geometric properties of a previously binarised welding arc area. During the tests the following topological features were taken into consideration: shape factor, area, Feret coefficient, circumference, Malinowska coefficient, longer diagonal and shorter diagonal. The third type was composed of features resulting from the analysis of the horizontal profile of the welding arc area. The horizontal profile passing through the weld pool area has a pseudosymmetric character resulting from welding process properties. Disorders in the profile symmetry may indicate the instability of a welding process. This assumption made it possible to indicate the profile features which can be the widths between the abscissas of characteristic points, where characteristic points are the extrema of the horizontal profile passing through the maximum value image pixel. In the tests, the following parameters were taken into consideration (Fig.7): left external width and right external width (LEW, REW); left and right internal width (LIW, RIW); central width (CW); left and right half width (LHW, RHW) as well as total width (TW). The values of determined features were applied to determine diagnostic signals used for recognising the state of a welding process.

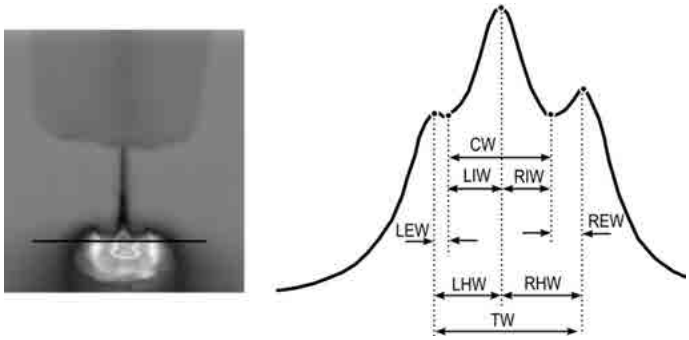

Fig. 7. Manner of determining features basing on the linear profile of post-fusion image pixel values

The diagnostic signals determined as a result of post-fusion image analysis were estimated using the following point statistical features known in technical diagnostics: average value, root-mean-square value, peak-to-peak value or kurtosis. The obtained numerical values of signal features were the basis for the operation of recognising welding process states by way of classification. Figure 8 presents the scheme of obtaining models describing various welding process states.

Recognition of welding process state

The recognition of a welding process state involved the development of models describing each of the welding process states simulated during the experiment. Each model was a one-dimensional vector consisting of the values of the features determined for a given welding process. The models were used to form both a training set and a testing set, in accordance with principles of building and teaching classifiers.

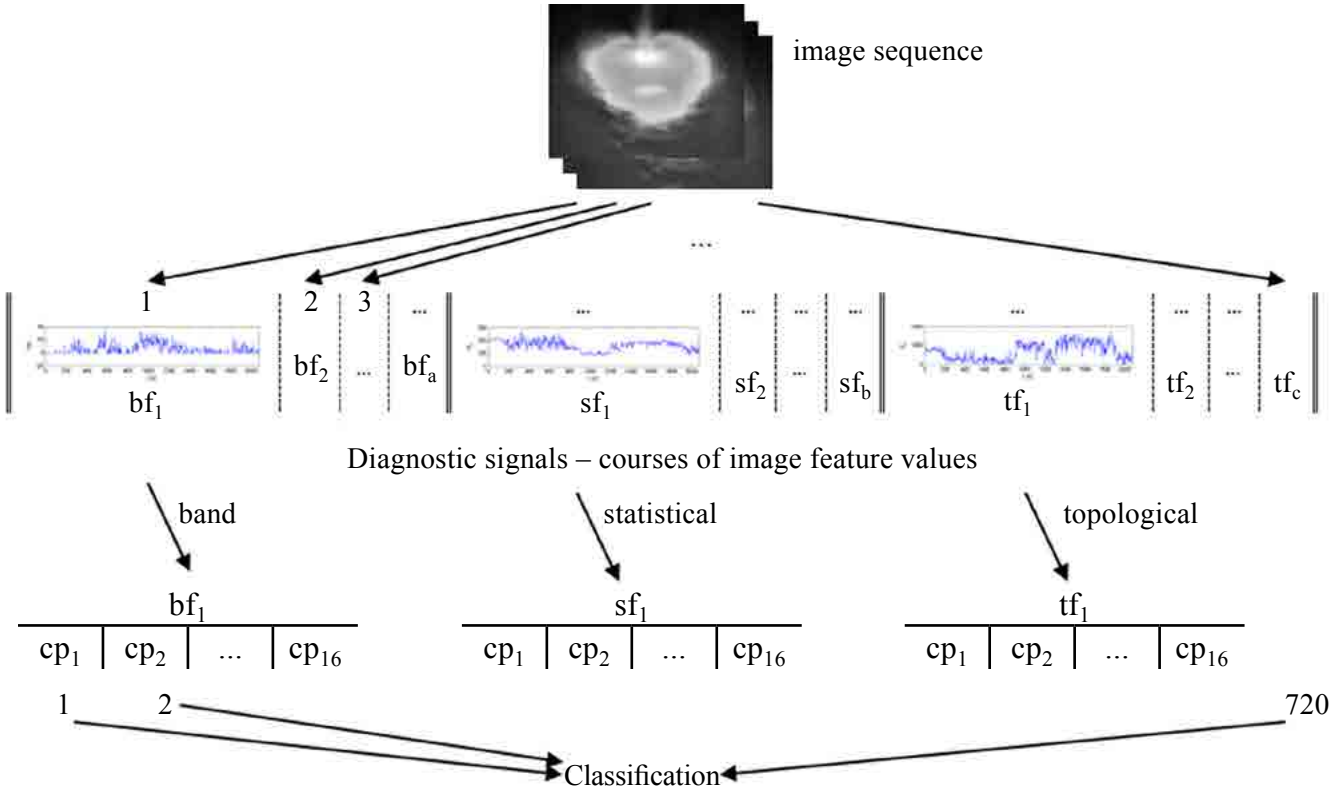

Fig 8. Scheme of obtaining models describing welding process

For the purpose of state recognition it was necessary to use a minimum distance classifier using the k-nearest neighbour algorithm, where k amounted to 7. The value of parameter k was selected experimentally on the basis of preliminary tests. The estimation of a classifier error was carried out using n-fold cross-validation (*leave-one-out*). In this method the process of training and testing is repeated N-times, where N is a number of teaching examples. In each iteration the teaching set has N-1 elements, whereas the testing set has one element. In this method each element of the set of teaching examples is a testing example. The method leave-one-out was used because of a not too numerous set of teaching examples. The relative number of correct assignments was used as a measure of state recognition efficiency:

$$e_{err} = \frac{N_g}{N} \quad (1)$$

where N_g is the number of properly recognised examples and N is the number of all examples in the teaching and testing sets. The process of state recognition was considered for two cases:

- classifier made an assignment to one of the states from z_0 to z_7, which means that both the examples, for which welding proceeded properly and those with simulated disturbances leading to welding imperfections were considered;
- classifier made an assignment to one of the states from z_1 to z_7, which means that only the examples with simulated disturbances leading to welding imperfections were considered; in other words a distinction between undesired states was made.

Prior to a state recognition, on the basis of the set of models determined on the basis of post-fusion images (FU), classification was also performed for the models determined separately for the thermographic images (IR) and images recorded in the range of visible radiation (TV). The models for the thermographic images and vision images were built on the same principle as in the case of

post-fusion images. The classification on the basis of separately determined features of the thermographic images and vision images made it possible to assess the usability of image fusion. Table 2 presents the values of classification efficiency for considered welding process states obtained for selected features and selected diagnostic signals determined on the basis of the sequence of thermographic images (IR), vision images (TV) and post-fusion images (FU)TV. The cases selected were those for which the average value of classification efficiency was the highest. The highest classification efficiency was achieved for the diagnostic signal obtained by determining the average value of the signal containing the values of the total width of a characteristic band (TW), calculated for the sequence of images received as a result of the fusion (FU).

Figure 9a presents the comparison of the maximum, minimum and medium (marked with a square) values of the classification efficiency for the diagnostic signals determined for individual sequences of images. The sequences of post-fusion images made it possible to obtain the highest values of classification efficiency $e_{err} = 0.59$, where the average value of efficiency is also higher than in the case of the diagnostic signals determined from the sequences of TV and IR images. Taking into consideration only the states representing the occurrence of welding imperfections (Fig. 9b) one can notice that the best results were obtained for the signals generated from the sequences of the post-fusion images, $e_{err} = 0.61$. Very poor results were obtained for the use of the signals obtained from the sequences of the thermographic images $e_{err} = 0.44$, with very similar average values.

Table 2. Classification efficiency in recognising individually identified welding process states for the classifier of the maximum total efficiency

Signal	State								Mean z_0-z_7	Mean z_1-z_7
	z_0	z_1	z_2	z_3	z_4	z_5	z_6	z_7		
IR Variance	0,91	0,17	0,86	0,29	0,71	0,17	0,43	0,00	0,37	0,44
TV RIW RMS	0,91	0,67	0,86	0,29	0,57	0,33	0,71	0,14	0,51	0,56
FU TW absolute mean	0,45	0,67	1,00	0,57	0,86	0,17	0,86	0,00	0,59	0,57

While analysing the achieved results one can also notice that for the images obtained as a result of fusion, the classification result for the state representing the properly conducted welding process is worse than the classification results obtained on the basis of the sequence of IR and TV images only. In the case of the states representing imperfections, the assessment of post-fusion images significantly improved classification efficiency. The states of special interest are z5 and z7, for which very low results of classifier efficiency obtained for the thermographic images are directly reflected in the results obtained for the classifiers based on the signals generated from the sequence of post-fusion images.

Using appropriate methods for the selection of features it is possible to select features enabling (in many cases) error-free recognition of some states. Such an approach makes it possible to increase the efficiency of classification and thereby identify states which are most difficult to recognise. The tests resulted in increasing the efficiency of classification using groups of seven classifiers, each of which distinguished whether a given case belonged to one of the identified classes or not. Each classifier could op-

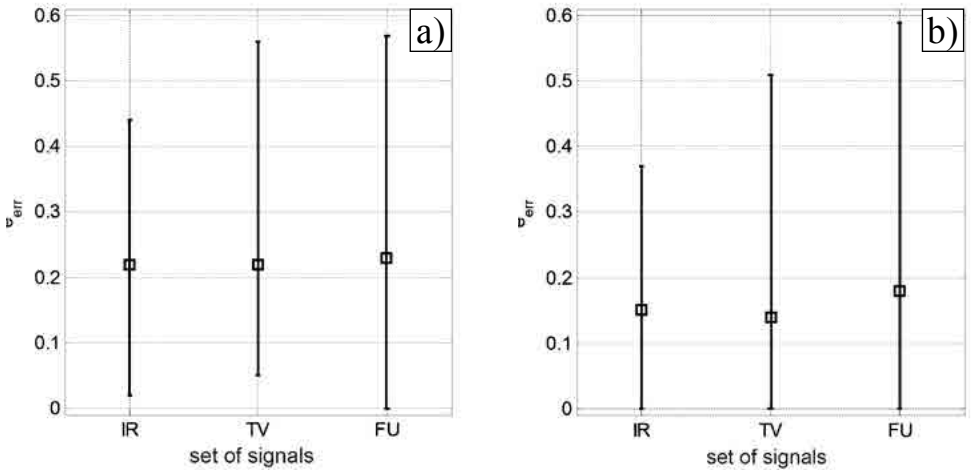

Fig. 9. Classification efficiency values:
a) during recognising all identified states,b) during recognising states with welding imperfections (set of signals; set of signals)

erate on a different previously determined feature. Table 3 presents the maximum classification values obtained for states under consideration. The error-free recognition of states z_0, z_1, z_2 and z_4 was obtained for the models created from the features of all considered diagnostic signals. States z_6 and z_7 created as a result of welding arc instability and improper weld groove geometry were characterised by the lowest recognisability. It was not possible to achieve error-free recognition for any of these states.

Table 3. Classification efficiency in recognising individually identified welding process states (maximum values)

Signal	State							
	z_0	z_1	z_2	z_3	z_4	z_5	z_6	z_7
IR	1,00	1,00	1,00	0,86	1,00	1,00	0,86	0,86
TV	1,00	1,00	1,00	0,86	1,00	0,67	0,71	0,71
FU	1,00	1,00	1,00	1,00	1,00	0,83	0,86	0,86

Summary

Recognising state changes is the primary diagnostic objective often obtained by way of model recognition. For this reason obtaining proper diagnostic signals being the basis for the generation of models is an important, yet complicated task. Making use of too many diagnostic signals is not advantageous either, and therefore it is advisable to maximise the information content of such signals. In the case of a multi-mode vision observation the reduction of the number of sequences to be analysed, and thus the limitation of the number of determined diagnostic signals can be achieved by merging images using image fusion methods.

The conducted tests revealed that the sequences of images obtained as a result of the fusion of IR (thermographic) and TV (recorded in visible radiation) images can be the basis for obtaining better and more important diagnostic signals than those which can be obtained by analysing the sequences of input images (IR and TV) for the fusion process. The manner of image analysis significantly affects the quality of the obtained diagnostic signals. All imperfections such as, for instance, image mismatching related to possible momentary and sudden displacements of cameras during image acquisition significantly deteriorate the final state recognition quality. It should also be noted that the selection of a feature used to describe the whole sequence significantly affects the final diagnostic outcome. The obtained results indicate that the use of image fusion enables the efficient identification of various welding imperfection generated during welding.

Research work financed from funds for science in the years 2009-2012

References

1. Burt, P., and Kolczynski, P (1993).“Enhanced image capture through fusion”, paper presented at *Computer Vision 4th International Conference*, Proceedings, pp. 173–182.
2. Jamrozik, W., and Fidali, M. (2011). Metody dopasowania termogramów i obrazów wizyjnych dla dynamicznie zmieniającej się struktury obserwowanej sceny. *Measurement, Automation and Monitoring*, 57 (10), pp.1134-1137.
3. Jamrozik, W., and Fidali, M. (2012). “Evaluation of the suitability of IR and TV image aggregation algorithms for the purposes of welding process assessment”, paper presented at *11th Quantitative InfraRed Thermography Conference*, Naples, Italy, 11-14 June.
4. Jamrozik, W., and Fidali M. (2011). Estimation of image fusion methods for purposes of vision monitoring of industrial process. *Measurement, Automation and Monitoring,* 57 (09), pp. 993-996.
5. Kim, Y. S., Lee, J. H., and Ra, J. B. (2008). Multi-sensor image registration based on intensity and edge orientation information. *Pattern Recognition*, 41, pp. 3356-3365.
6. Rockinger, O. (1997). “Image Sequence Fusion Using a Shift Invariant Wavelet Transform”, paper presented at *International Conference on Image Processing*, Proceedings, vol.3, pp. 288-291.
7. Nandhitha, N. M., Manoharan, N., Rani, B.S., Venkataraman, B., Sundaram, P. K., and Ra, J.B. (2006). “Automatic Detection and Quantification of Incomplete Penetration in TIG Welding Through Segmentation and Morphological Image Processing of Thermographs”, paper presented at *National Seminar on Non-Destructive Evaluation,* Hyderabad, 7-9 December, Proceedings, pp. 17-22.